

# Optical and Electrical Simulation of $\text{CH}_3\text{NH}_3\text{PbI}_3$ -Based Perovskite Solar Cells

Elham Karimi, Seyed Mohamad Bagher Ghorashi\*, and Maryam Hashemi

Department of Physics, Faculty of Physics, University of Kashan, Kashan, Iran.

\*Corresponding author : [mghorashi@kashanu.ac.ir](mailto:mghorashi@kashanu.ac.ir)

Regular paper: Received: Oct. 31, 2018, Revised: May. 27, 2019, Accepted: Jun. 29, 2019,  
Available Online: June. 30, 2020, DOI: 10.29252/ijop.14.1.57

**ABSTRACT**— Recently, organo–metal halide perovskites have attracted much attention of the scientific community relating to their successful application in the absorber layer of low-cost solar cells. However, enough is known about the material and device properties, to realize that much remains to be learned.

In this paper, the electrical and optical properties of perovskite solar cells are investigated using the COMSOL Multiphysics simulation program. It is a study of the influences of carrier diffusion length ( $L$ ), dielectric constant ( $\epsilon_r$ ), the valence band offset (VBO) of absorber/hole transport materials (HTM) and illumination intensity on fill factor (FF), short-circuit current density ( $J_{SC}$ ), performance (PCE), and open-circuit voltage ( $V_{OC}$ ). Also, J-V characteristics are calculated for different  $\epsilon_r$  values. The simulation results point to the great dependence of efficiency on the carrier diffusion length of absorber layers. It is shown that, to obtain a high rate of efficiency, the relative permittivity should not be higher than 45.

**KEYWORDS:** Perovskite solar cells, Fill Factor, Power Conversion Efficiency, Simulation.

## I. INTRODUCTION

Mixed organic–inorganic halide perovskites solar cells are encouraging as future-generation photovoltaic tools due to their benefits such as easy processing, high cost-effectiveness and efficiency [1, 2]. Principally, perovskite solar cells can serve as planar-junction devices or mesoscopic-junction devices. A performance rate of over 15% has been obtained for the two categories [3-5].

Proposing that the mesoporous is not the prerequisite for high performance [6].

The highest performance of 19.3% is attained by optimizing the expansion atmosphere and the band positions [7-9]. The dielectric and optical features of perovskites are vital to optimize the structure of perovskite solar cells [10,11]. It was obtained that the dielectric constant of perovskite displayed a frequency dependency and temperature [12-14].

In 1994, a broadly cited optical frequency dielectric constant of 6.5 was reported for perovskites. It was computed from diffuse powder reflection, and currently declined to 5.06 inferred from detailed analysis of transmittance and reflectance of films [15-17]. A great dielectric constant has been also reported for the iodide recently, in which another extra factor of 1000 is made under the illumination of one sun when measured at very low frequencies (<1 Hz) [18-20].

Detailed studies of the dark IV features of perovskite solar cells have suggested that the low-frequency relative permittivity of perovskites is like that of HTL [21]. However, the impact of dielectric constant on light characteristics is not known yet. Highly efficient perovskite solar cells generally benefit from organic hole transport materials (HTMs) which are often costly and have bottom low hole mobility [22]. Perovskite solar cells based on inorganic p-type semiconductors are expanded, but their performance is lower than that of cells based

on organic materials.<sup>14</sup> This shows the valence band offset (VBO = E<sub>V,perovskite</sub> - E<sub>V,HTM</sub>) of the absorber/HTM layers should be significant.

The literature on the topic is growing, both in fully simulating and empirical forms. Simulation studies provide deep insights into the function of cells and the restrictions to their efficiency. Those studies are generally appropriate for monitoring, fast characterization and prediction of panel efficiency [23, 24].

A simulation program is very beneficial for clarifying the key roles of different parameters in final operations. In this paper, to determine the action mechanism of perovskite devices, theoretical analyses are performed of the influence of carrier diffusion length, VBO and dielectric constant on the photovoltaic parameters of perovskite solar cells. The COMSOL Multiphysics simulation software is used for both electrical and optical responses [25].

## II. DEVICE SIMULATION PARAMETERS

COMSOL is a window application program, developed at the University of Harford with which the user can set the parameters or in which the results are calculated [25]. COMSOL analyses the physics of the model and it explains the recombination profiles, electric field distribution, carrier transport mechanism and individual current densities. The continuity equations of electrons and holes are:

$$\frac{1}{q} \frac{dJ_n}{dx} = R_n(x) - G(x) \quad (1)$$

$$\frac{1}{q} \frac{dJ_p}{dx} = G(x) - R_p(x) \quad (2)$$

where,  $J_n$  is Electron Current Density,  $J_p$  is Hole Current Density and  $R$  is generation rate.

The Drift and Diffusion Equations are:

$$J_n = \frac{I_n}{A} = -nqv_n E + qD_n \nabla n \quad (3)$$

$$J_p = \frac{I_p}{A} = -pqv_p E - qD_p \nabla p \quad (4)$$

where,  $D_n$  is electron diffusion coefficient,  $v_n$  is electron mobility and  $v_p$  is Hole mobility.

Figure 1 explains the simulation process using COMSOL.

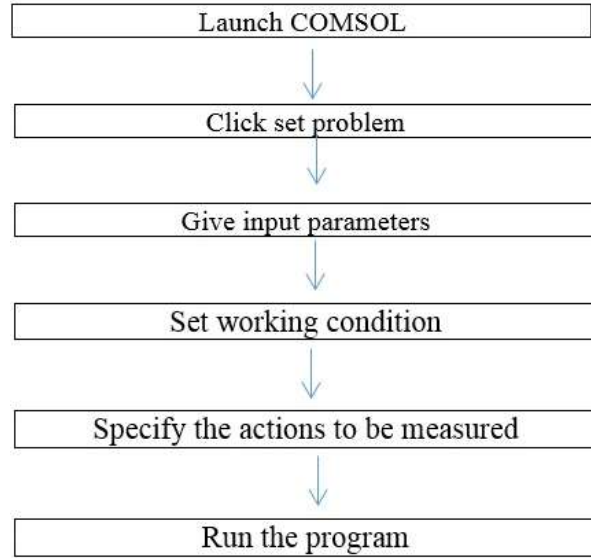
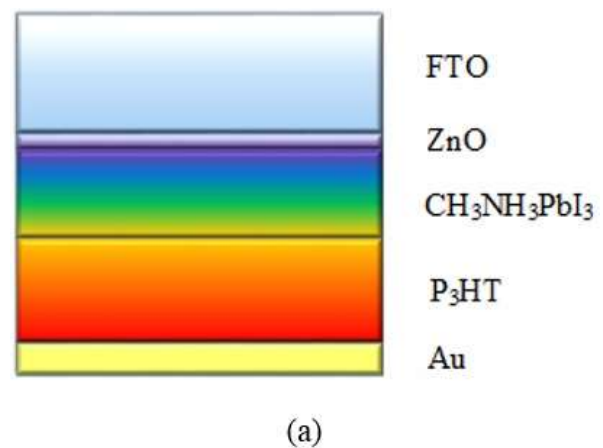


Fig. 1. COMSOL working procedure.

A simulation structure was devised for n-i-p perovskite solar cells. As displayed in Fig. 2, the specifications included FTO (500 nm)/ZnO (ETM layer, 50 nm)/CH<sub>3</sub>NH<sub>3</sub>PbI<sub>3</sub> (absorber layer, 400 nm)/P<sub>3</sub>HT (HTM layer, 350 nm)/Au (100 nm). The standard AM1.5G spectrum was presented as the accident light source, and the  $k$ ,  $n$  values of the stack as well as FTO, ZnO, CH<sub>3</sub>NH<sub>3</sub>PbI<sub>3</sub>, P<sub>3</sub>HT, and Au values were derived from the literature [26].



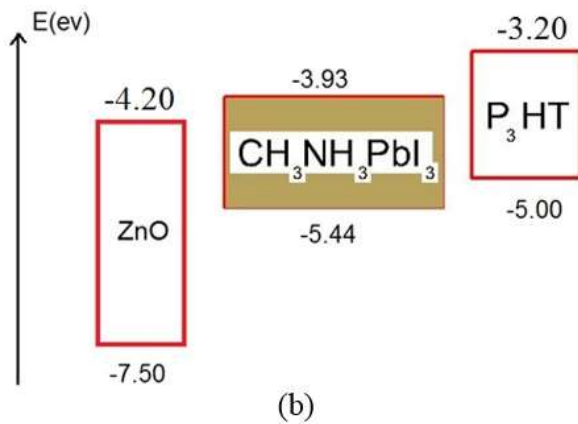


Fig. 2. (a) Schematic diagram of the perovskite solar cells, (b) Energy levels of different layers of the perovskite solar cells

The photo-generation rate obtained through the optical computation was used to determine the electrical characteristics, where only the three layers of n-type ZnO,  $\text{CH}_3\text{NH}_3\text{PbI}_3$  and p-type  $\text{P}_3\text{HT}$  were taken into consideration. The simulation parameters are presented in Table 1 [27-30].

**Table 1.** Semiconductor parameters used for the simulation

	ZnO [27-28]	$\text{CH}_3\text{NH}_3\text{PbI}_3$ [29]	$\text{P}_3\text{HT}$ [30]
Thickness (nm)	50	400	350
$E_g$ (eV)	3.3	1.5	1.8
$X$ (eV)	4.6	3.9	3.9
$\epsilon_r$	9	6.5	3
$N_C$ ( $\text{cm}^{-3}$ )	$2.2 \times 10^{18}$	$2.5 \times 10^{20}$	$10^{20}$
$N_V$ ( $\text{cm}^{-3}$ )	$1.8 \times 10^{19}$	$2.5 \times 10^{20}$	$10^{20}$
$\mu_e$ ( $\text{cm}^2/\text{Vs}$ )	100	50	$10^{-4}$
$c$ ( $\text{cm}^2/\text{Vs}$ )	25	50	$10^{-4}$
$N_D$ ( $\text{cm}^{-3}$ )	$10^{18}$		
$N_A$ ( $\text{cm}^{-3}$ )	--	$10^{13}$	$10^{16}$

Here,  $\epsilon_r$  is the relative permittivity,  $N_D$  and  $N_A$  denote the donor and acceptor densities,  $X$  refers to the electron affinity,  $N_V$  and  $N_C$  are the effective densities of the states of valence and conduction bands respectively,  $E_g$  is the band gap energy, and  $\mu_e$  and  $\mu_h$  are the mobility rates of electrons and holes respectively.

Ideal Ohmic and Schottky contacts with the surface recombination rate of  $10^7$   $\text{cm/s}$  were used in the case of back and front contacts.

information on efficiency, such as:  $J_{SC}$ ,  $V_{OC}$ , PCE, FF, J-V curve and etc. can all be attained for the optimization of perovskite solar cells designs.

Finally, information on efficiency, including  $J_{SC}$ ,  $V_{OC}$ , PCE, FF, J-V curve and etc. can all be obtained for the optimization of perovskite solar cells designs.

### III. RESULTS AND DISCUSSION

The spectral dependence of the absorptance of perovskite solar cells on the thickness of their absorber layers is shown in Fig. 3.

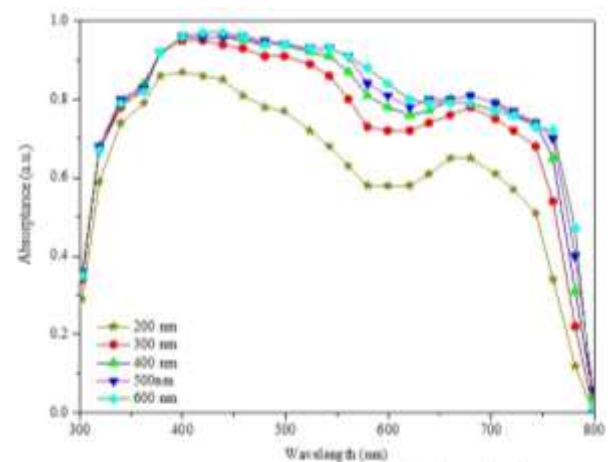


Fig. 3. Spectral affiliation of the light attracted by absorber layers with different thicknesses

The absorptance is enhanced quickly with the increase of the absorber thickness, and it reaches saturation for a thickness of more than 400. The integrated absorptance of absorber layers with different thicknesses between 200 and 600 nm is displayed in Fig. 4(a). It increases with the increase of the absorber layer thickness, and a value of upper 0.75 is obtained at 600 nm. Also, the generation current, where the photo-generated carriers are prepared without recombination, i.e. the theoretical maximum current, is enhanced with an increase in the absorber layer thickness and reaches around  $21 \text{ mA/cm}^2$  at 600 nm, as shown in Fig. 4(b).

Then illumination intensity was investigated as displayed in Fig. 5. To design the J-V curves of the cells, different illumination intensities were tried. The results show that, with the

increase of illumination intensity,  $J_{SC}$  would increase but  $V_{OC}$  would remain almost unchanged.

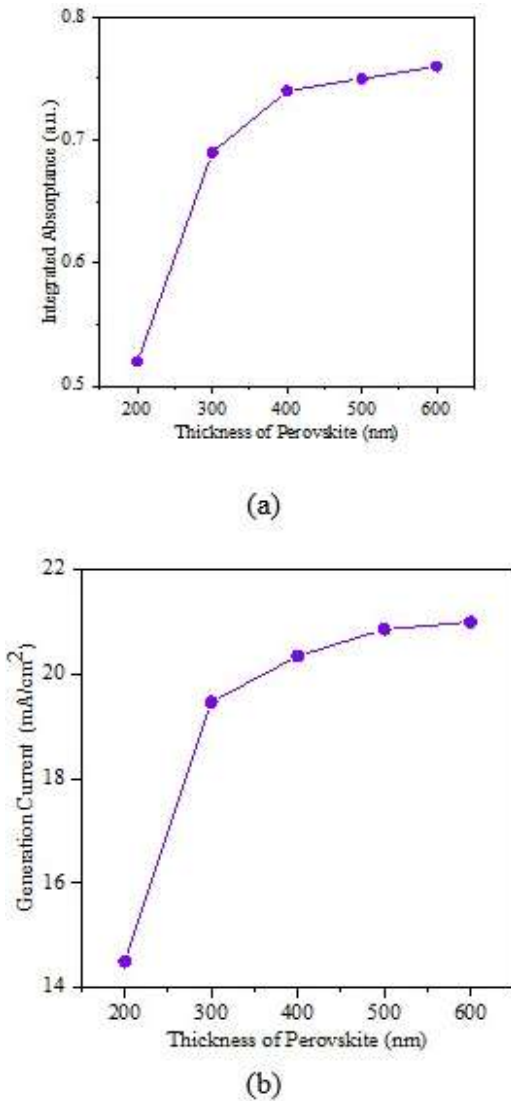


Fig. 4. Effect of absorber thickness on (a) integrated absorbance and (b) generation current

The absorber quality, namely carrier diffusion length for hole ( $L_p$ ) and electron ( $L_n$ ), is the main parameter of the efficiency of perovskite solar cells. The  $L_n$  of 100 nm estimated from the single-step solution-processed perovskite thin films was the minimum value, but it increased by one order (i.e.,  $>1$   $\mu\text{m}$ ) with Cl doping [19]. Furthermore, high crystalline films were entrusted by vapor deposition methods and the sequential, propose that the  $L_n$  as in the scale 100 nm.

In addition, high crystalline films were deposited by the sequentia and vapor

deposition methods, suggesting that the  $L_n$  was in the scale of hundreds of nanometers.

In addition, an efficiency rate of higher than 12% was gained in perovskite solar cells with a thickness about 300 nm, denoting that maximizing the quality of absorber films can lead to  $L_n$  and  $L_p > 300$  nm [30-33].

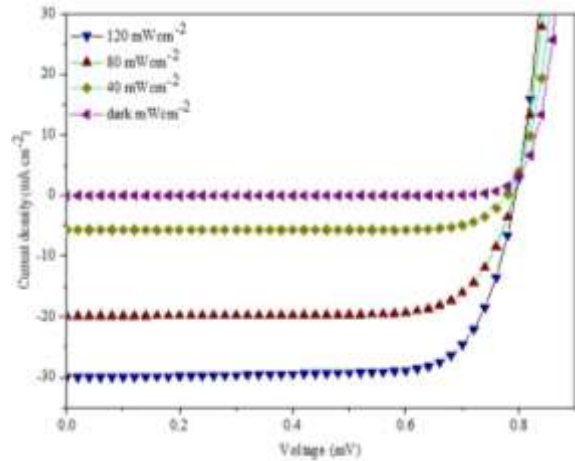


Fig. 5. J–V curves of the perovskite solar cells simulated with different illumination intensity values

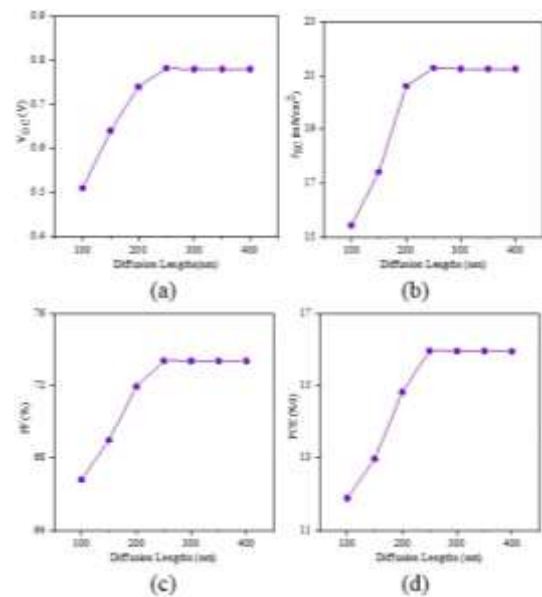


Fig. 6. Effect of the diffusion lengths ( $L$ ) of perovskite on (a)  $V_{OC}$  and (b)  $J_{SC}$  and (c) FF and (d) PCE.

The plot of the PV parameters versus the carrier diffusion length of the perovskite layers is shown in Fig.6. The  $L$  changed from 100 nm to 400nm. In this study,  $L_p$  and  $L_n$  are identical. It was observed that, with the



increase of the absorber diffusion length, i.e. with the improvement of the film quality,  $J_{SC}$ ,  $V_{OC}$ , FF and PCE increased. This increase was due to the suppression of recombination. And then more  $L=250$  nm they are constant. It means that, at  $L=250$  nm, the values PCE = 15.9%,  $J_{SC}= 21.2\text{mA/cm}^2$ ,  $V_{OC}= 0.78$  V and FF = 74.2% could be obtained.

If the absorber thickness is too low, full light absorption does not occur and the cell performance is low. When the absorber thickness is increased, the PCE is improved gradually. Once the absorber layer is too thick, it is not possible to collect the photo-generated carriers effectively because, before they are recombined, they must move through the absorber to reach the layers that collect them. The role of the charge diffusion length is critical in designing the thickness and structure of the perovskite layer. The effect of the absorber layer thickness on the performance of perovskite solar cells with different charge carrier diffusion lengths is displayed in Fig. 7.

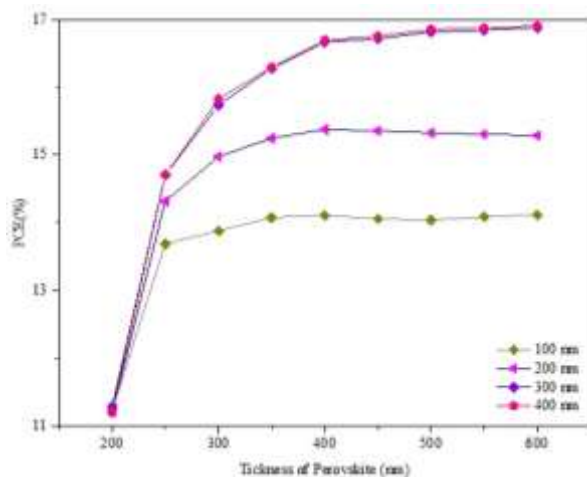


Fig. 7. Effect of the absorber thickness on PCE with different diffusion lengths.

As it can be seen, the performance is enhanced with the increase of the absorber thickness, but, when the perovskite thickness is above 400 nm, the performance is almost constant.

The influence of the dielectric constant on the performance of the perovskite solar cells was evaluated by the change from 5 a.u. to 135 a.u. versus the PV parameters. The results are given in Fig. 8.

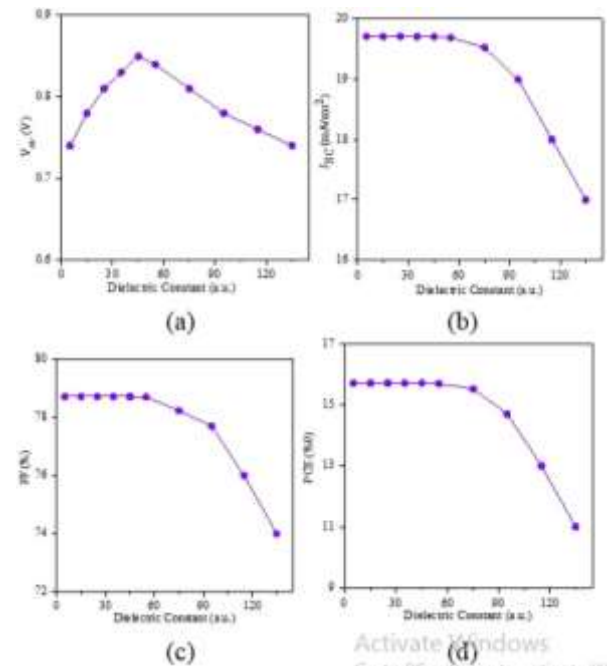


Fig. 8. Effect of the dielectric constant ( $\epsilon_r$ ) of perovskite on (a)  $V_{OC}$  and (b)  $J_{SC}$  and (c) FF and (d) PCE.

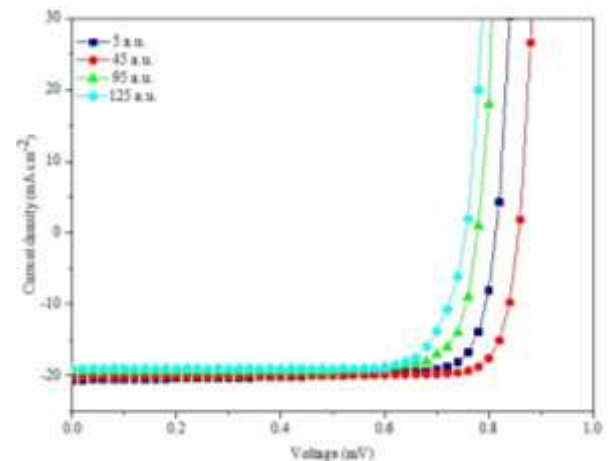


Fig. 9. J-V curves of the perovskite solar cells simulated with different dielectric constant values.

According to the figure, with the increase of  $\epsilon_r$  to 45 a.u.,  $J_{SC}$ , FF and PCE values remain unchanged. Then, with further increase of  $\epsilon_r$ , those values decrease. As for  $V_{OC}$ , however, it first increases with the increase of  $\epsilon_r$  to 45 a.u. and then decreases with higher  $\epsilon_r$ . Also, as presented in Fig. 9, the influence of different dielectric constants on the J-V characteristics of the solar cells was examined. The same result was reached in this examination; with an increase of  $\epsilon_r$  up to 45 u.a.,  $V_{OC}$  increases and then decreases with more raise in  $\epsilon_r$ .

The effect of the band offset values of the absorber/HTM interface on the performance of the perovskite solar cells was calculated according to the PV parameters. The results are displayed in Fig. 10. As the figure shows, for  $\text{VBO} < 0$ , with an increase of VBO, the values of  $V_{OC}$ , FF, PCE increase, while the short-circuit current density remains almost unchanged.

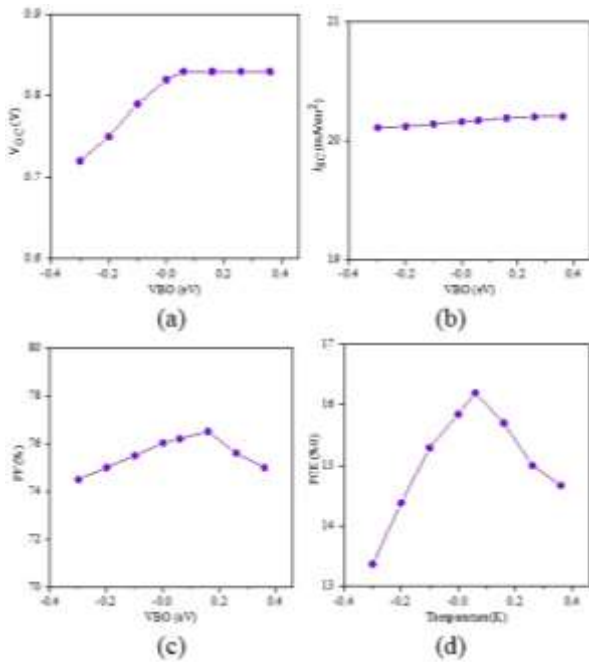


Fig. 10. Effect of valence band offset (VBO) on (a)  $V_{OC}$  and (b)  $J_{SC}$  and (c) FF and (d) PCE

In the case of  $\text{VBO} = 0.13$ , Fig. 10 suggests a high performance. With further enhancement of VBO, a double-diode like a curvature is presented, resulting in low FF but similar  $V_{OC}$ . However, VBO is negative for most HTMs, such as  $\text{CuSCN}$  (-0.13 eV) and  $\text{CuI}$  (-0.23 eV) [34-36]

#### IV. CONCLUSION

In summary, planar PSCs have been simulated, which calculates both the optical and electronic responses of a solar cell structure. The effect of carrier diffusion length, dielectric constant, the valence band offset of absorber/HTM and illumination intensity on the PV parameter of perovskite solar cells as well as the spectral affiliation of the light attracted by absorber layers with different thicknesses. Also, the effect of absorber

thickness on the integrated absorbance and generation current was calculated. According to the simulation results, the optimal carrier diffusion length, absorber layer thickness, VBO and dielectric constant were 250 nm, 400nm, 0.13 and 45 a.u. respectively. Also, the optimal values and the calculated photovoltaic parameters were  $V_{OC} = 0.81$  V,  $J_{SC} = 20.04$  mA/cm<sup>2</sup>, PCE = 15.36% and FF = 75.03%. Based on this study, some insight is provided into the working mechanism of perovskite devices and the properties of perovskite films. This can be of benefit for designing better perovskite solar cells.

#### REFERENCES

- [1] M.J. Taghavi, M. Houshmand, M.H. Zandi, and N.E. Gorji, "Modeling of optical losses in perovskite solar cells," *Superlattice. Microst.* Vol. 97, pp. 424-428, 2016.
- [2] V.J. Babu, S. Vempati, S. Sundarrajan, M. Sireesha, and S. Ramakrishna, "Effective nano structured morphologies for efficient hybrid solar cells," *Sol. Energy*, Vol. 106, pp. 1-22, 2014.
- [3] J. Burschka, N. Pellet, S.J. Moon, R. Humphry, P. Gao, M.K. Nazeeruddin, and M. Gratzel, "Sequential deposition as a route to high-performance perovskite-sensitized solar cells," *Nature*. Vol. 499, pp. 316-319, 2013.
- [4] Q. Chen, H. Zhou, Z. Hong, S. Luo, H.S. Duan, H.H. Wang, Y. Liu, G. Li, and Y. Yang, "Planar heterojunction perovskite solar cells via vapor-assisted solution process," *J. Am. Chem. Soc.* Vol. 136, pp. 622-625, 2014.
- [5] M.A. Green, A. Baillie, and H.J. Snaith, "The emergence of perovskite solar cells," *Nat. Photonics*, Vol. 8, pp. 506-514, 2014.
- [6] X. Xu, X. Wang, W. Gu, S. Quan, and Z. Zhang, "Study on influences of CdZnS buffer layer on CdTe solar cells," *Superlattices Microstruct.* Vol. 109, pp. 463-469, 2017.
- [7] O.K. Simya, A. Mahaboobatcha, and K. Balachander, "Compositional grading of

- CZTSSe alloy using exponential and uniform grading laws in SCAPS-ID Simulation,” *Superlattices Microstruct.* Vol. 92, pp. 285-293, 2016.
- [8] O.K. Simya, A. Mahaboobbatcha, and K. Balachander, “A comparative study on the performance of Kesterite based thin film solar cells using SCAPS simulation program,” *Superlattices Microstruct.* Vol. 82, pp. 248–261, 2015.
- [9] E. Karimi and S.M.B. Ghorashi, “Investigation of the Influence of Different Hole-Transporting Materials on the Performance of Perovskite Solar Cells,” *Optick*, Vol. 16, pp. 650-658, 2016.
- [10] S.R. Meher, L. Balakrishnan, and Z.C. Alex, “Analysis of Cu<sub>2</sub>ZnSnS<sub>4</sub>/CdS based photovoltaic cell: A numerical simulation approach,” *Superlattices. Microstruct.* Vol. 100, pp.703–722, 2016.
- [11] W.I. Nam, Y.J. Yoo, and Y.M. Song, “Geometrical shape design of nanophotonic surfaces for thin film solar cells,” *Opt. Express*, Vol. 24, pp. A1033–A1044, 2016.
- [12] X. Jia, L. Shen, Y. Liu, W. Yu, X. Gao, Y. Song, W. Guo, S. Ruan, and W. Chen, “Performance improvement of inverted polymer solar cells thermally evaporating CuI as an anode buffer layer,” *Synth. Met.* Vol. 198, pp. 1–5, 2014.
- [13] Y. Jiang, M.A. Green, R. Sheng, and A. Baillie, “Room temperature optical properties of organic–inorganic lead halide perovskites,” *Sol. Energy Mater. Sol. Cells*, Vol. 137, pp. 253–257, 2015.
- [14] E.J. Juarez, R.S. Sanchez, L. Badia, G.Garcia, Y.S. Kang, L. Mora, and J. Bisquert, “Photoinduced giant dielectric constant in lead halide perovskite solar cells,” *J. Phys. Chem. Lett.* Vol. 5, pp. 2390–2394, 2014.
- [15] L. Kavan and M. Graetzel, “Highly efficient semiconducting TiO<sub>2</sub> photoelectrodes prepared by aerosol pyrolysis,” *Electrochim. Acta*, Vol. 40, pp. 643–652, 1995.
- [16] H.S. Kim, C.R. Lee, J.H. Im, K.B. Lee, T. Moehl, A. Marchioro, S.J. Moon, R. Humphry, J. H. Yum, J.E. Moser, M. Graetzel, and N.G. Park, “Lead iodide perovskite sensitized all-solid-state submicron thin film mesoscopic solar cell with efficiency exceeding 9%,” *Sci. Rep.* Vol. 2, pp. 591 (1-7), 2012.
- [17] M.M. Lee, J. Teuscher, T. Miyasaka, T.N. Murakami, and H.J. Snaith, “Efficient hybrid solar cells based on meso-structured organometal halide perovskites,” *Science*, Vol. 338, pp. 643–647, 2012.
- [18] X. Li, N.P. Hylton, V. Giannini, K.H. Lee, N.J. Daukes, and S.A. Maier, “Bridging electromagnetic and carrier transport calculations for three-dimensional modelling of plasmonic solar cells,” *Opt. Express*, Vol. 19, pp. 888–896, 2011.
- [19] D. Liu and T.L. Kelly, “Perovskite solar cells with a planar heterojunction structure prepared using room-temperature solution processing techniques,” *Nature Photon*, Vol. 8, pp. 133–138, 2014.
- [20] A. Asadollahbaik, S.A. Boden, M.D.B. Charlton, D.N.R. Payne, S. Cox, and D.M. Bagnall, “Reflectance properties of silicon moth-eyes in response to variations in angle of incidence, polarisation and azimuth orientation,” *Opt. Express*, Vol. 22, pp. A402–A415, 2014.
- [21] M. Liu, M.B. Johnston, and H.J. Snaith, “Efficient planar heterojunction perovskite solar cells by vapour deposition,” *Nature*, Vol. 501, pp. 395–398, 2013.
- [22] P. Loper, M. Stuckelberger, B. Niesen, J. Werner, M. Filipic, S.J. Moon, J.H. Yum, M. Topic, S.D. Wolf, and C. Ballif, “Complex refractive index spectra of CH<sub>3</sub>NH<sub>3</sub>PbI<sub>3</sub> perovskite thin films determined by spectroscopic ellipsometry and spectrophotometry,” *J. Phys. Chem. Lett.* Vol. 6, pp. 66–71, 2015.
- [23] L. Liu, Y. Huo, K. Zhao, T. Zhao, and Y. Li, “Broadband absorption enhancement in plasmonic thin-film solar cells with

- grating surface,” *Superlattices Microstruct.* Vol. 86, pp. 300-305, 2015.
- [24] T. Minemoto and M. Murata, “Theoretical analysis on effect of band offsets in perovskite solar cells,” *Sol. Energy Mater. Sol. Cells*, Vol. 133, pp. 8–14, 2015.
- [25] A.J. Moule, H.J. Snaith, M. Kaiser, H. Klesper, D.M. Huang, M. Gratzel, and K. Meerholz, “Optical description of solid-state dyesensitized solar cells,” *J. Appl. Phys.* Vol. 106, pp. 073-111, 2009.
- [26] N. Yamamuro, T. Matsuo, and H. Suga, “Dielectric study of CH<sub>3</sub>NH<sub>3</sub>PbX<sub>3</sub>, (X = Cl, Br, I),” *J. Phys. Chem. Solids*, Vol. 53, pp. 935–939, 1992.
- [27] D. Poplavsky and J. Nelson, “Nondispersive hole transport in amorphous films of methoxy-spirofluorene-arylamine organic compound,” *J. Appl. Phys.* Vol. 93, pp. 341-349, 2003.
- [28] H.J. Snaith and M. Gratzel, “Electron and hole transport through mesoporous TiO<sub>2</sub> infiltrated with spiro-MeOTAD,” *Adv. Mater.* Vol. 19, pp. 3643–3647, 2007.
- [29] E. Karimi and S.M.B. Ghorashi, “Simulation of perovskites solar cell with P<sub>3</sub>HT hole-transporting materials,” *J. Nano photonics*. Vol. 11, pp. 1-15, 2017.
- [30] T. Leijtens, L.M. Herz, A. Petrozza, and H.J. Snaith, “Electron–hole diffusion lengths exceeding 1 micrometer in an organometal trihalide perovskite absorber,” *Science*, Vol. 342, pp. 341–344, 2013.
- [31] K. Tanaka, T. Minemoto, and H. Takakura, “Analysis of heterointerface recombination by Zn<sub>1-x</sub>Mg<sub>x</sub>O for window layer of Cu(In, Ga) Se<sub>2</sub> solar cells,” *Sol. Energy*, Vol. 83, pp. 477–479, 2009.
- [32] S. Wenger, M. Schmid, G. Rothenberger, A. Gentsch, M. Gratzel, and J.O. Schumacher, “Coupled optical and electronic modeling of dye-sensitized solar cells for steady-state parameter extraction,” *J. Phys. Chem. C*, Vol. 115, pp. 10218–10229, 2011.
- [33] Z. Xiao, Q. Dong, C. Bi, Y. Shao, Y. Yuan, and J. Huang, “Solvent annealing of perovskite-induced crystal growth for photovoltaic-device efficiency enhancement,” *Adv. Mater.* Vol. 26, pp. 6503–6509, 2014.
- [34] Z. Xiao, C. Bi, Y. Shao, Q. Dong, Q. Wang, Y. Yuan, C. Wang, Y. Gao, and J. Huang, “Efficient, high yield perovskite photovoltaic devices grown by interdiffusion of solution-processed precursor stacking layers,” *Energy Environ. Sci.* Vol. 7, pp. 2619–2623, 2014.
- [35] G.C. Xing, N. Mathews, S.Y. Sun, S.S. Lim, Y.M. Lam, M. Gratzel, S.M. haisalkar, and T.C. Sum, “Long-range balanced electron- and hole-transport lengths in organic–inorganic CH<sub>3</sub>NH<sub>3</sub>PbI<sub>3</sub>,” *Science*, Vol. 342, pp. 344–347, 2013.
- [36] H.P. Zhou, Q. Chen, G. Li, S. Luo, T.B. Song, H.S. Duan, Z.R. Hong, J.B. You, Y.S. Liu, and Y. Yang, “Interface engineering of highly efficient perovskite solar cells,” *Science*, Vol. 345, pp. 542–546, 2014.



**Maryam Hashemi** was born in Tehran, Iran, in 1983. She received her MSc. degree from Physics Faculty in University of Shiraz, Iran in 2011. She worked for her M.Sc. thesis on the Fiber Optics. She is now PhD student and works on Solar cell based on perovskite and Chalcogenide absorbers.





**Seyed Mohamad Bagher Ghorashi** was born in Shahreza, Iran, in 1978. He received the B.E. degree in Physics from the Yazd University, in 2000, and the M.S degree in Esfahan University, in 2004, and Ph.D degree from the Yazd University in 2011.

In 2011, he joined the Department of Physics, University of Kashan, as an Assistant Professor, His current research interests include Organic and Polymer Solar Cells, Perovskite Solar Cells, Thin Films, CIGS

Solar Cells, Electrochromic Glasses and OLED.



**Elham Karimi** was born in Esfahan, Iran. She received B.S from Kharazmi University, Iran in 2011. She received her Master's degree in Esfahan University, Iran in 2013. Currently, she is a Ph.D. candidate in Optics and Laser in the University of Kashan, Iran. Her research interest focuses on investigation on perovskite solar cells and organic solar cells.

**THIS PAGE IS INTENTIONALLY LEFT BLANK.**